

Evidence for Scattering-Dependent Multigap Superconductivity in $\text{Ba}_8\text{Si}_{46}$

Yves Noat, Tristan Cren, Pierre Toulemonde, Alfonso San Miguel,
François Debontridder, Vincent Dubost and Dimitri Roditchev
Institut des Nanosciences de Paris, Université Pierre et Marie Curie-Paris
6 and CNRS-UMR 7588, 4 place Jussieu, 75252 Paris, France

Institut Néel, CNRS et Université Joseph Fourier,
25 avenue des Martyrs, BP 166 F-38042 Grenoble cedex 9, France and
Laboratoire de Physique de la Matière Condensée et Nanostructures CNRS UMR-5586,
43 bld du 11 novembre 1918, 69622 Villeurbanne, Lyon, France

(Dated: April 19, 2021)

We have studied the quasiparticle excitation spectrum of the superconductor $\text{Ba}_8\text{Si}_{46}$ by local tunneling spectroscopy. Using high energy resolution achieved in Superconductor-Superconductor junctions we observed tunneling conductance spectra of a non-conventional shape revealing two distinct energy gaps, $\Delta_L = 1.3 \pm 0.1$ meV and $\Delta_S = 0.9 \pm 0.2$ meV. The analysis of tunneling data evidenced that Δ_L is the principal superconducting gap while Δ_S , smaller and more dispersive, is induced into an intrinsically non-superconducting band of the material by the inter-band quasiparticle scattering.

PACS numbers: 74.25.Gz, 74.72.Jt, 75.30.Fv, 75.40.-s

In their microscopic theory of superconductivity [1] Bardeen, Cooper and Schrieffer (BCS) predicted the existence of a single gap $\Delta = cte$ in the elementary excitation spectrum of a superconductor (SC). However, already in late 60s, some SCs from the A15 family did show anomalies in specific heat that could be attributed to the presence of several energy gaps [2, 3]. The existence of two energy gaps has also been suggested for Nb, Ta and V [4]. Recent discovery of the two distinct SC gaps in MgB_2 reported in specific heat [5] and Scanning Tunneling Microscopy/Spectroscopy (STM/STS) experiments [6, 7], with the excitation spectrum deviating from the BCS, strongly renewed the interest for non-standard SCs [8–11].

Among the covalent sp^3 materials, like silicon carbide or silicon (or carbon) diamond, the silicon clathrate $\text{Ba}_8\text{Si}_{46}$ appears to be a good candidate for a non-conventional superconductivity. This doped clathrate is formed by covalent Si_{20} and Si_{24} cages sharing their faces and filled with intercalated Ba atoms (for more details, see [12]). It has been shown that the superconductivity appearing in $\text{Ba}_8\text{Si}_{46}$ at $T_c = 8.1$ K [13–17] is mediated by phonons and is an intrinsic property of the sp^3 network formed by Si atoms [16]. Eight encaged Ba atoms per unit cell provide the charge carriers [18] resulting in a complex band structure with several bands crossing the Fermi level. Thus, one could expect the superconductivity to appear in two or more bands, and to depend on the inter-band scattering. Up to now however, the question remained a subject of controversy: K. Tanigaki et al. concluded on a conventional BCS superconductivity in $\text{Ba}_8\text{Si}_{46}$ [17], while tunneling spectroscopy data evidenced for an anisotropic order parameter [19], and recent results of specific heat measurements were reported to be consistent with two-gap superconductivity [11].

In this Letter we report the local tunneling spec-

troscopy (TS) of $\text{Ba}_8\text{Si}_{46}$ performed in the STM geometry. In order to enhance the energy resolution, we studied Superconductor-Vacuum-Superconductor (SIS) tunneling junctions formed by *in-situ* cleaved $\text{Ba}_8\text{Si}_{46}$ grains (used as STM tips) [6] and a clean surface of $2H\text{-NbSe}_2$ or, alternatively, another grain of $\text{Ba}_8\text{Si}_{46}$, used as a "sample". Statistical analysis of SIS spectra revealed two energy gaps to exist in $\text{Ba}_8\text{Si}_{46}$, a large one $\Delta_L = 1.3 \pm 0.1$ meV, giving a ratio $2\Delta_L/kT_c = 3.7 \pm 0.3$ matching the BCS value, and a smaller one $\Delta_S = 0.9 \pm 0.2$ meV. This apparent small gap is interpreted as being due to the inter-band scattering induced superconductivity in an intrinsically non-superconducting electronic band of $\text{Ba}_8\text{Si}_{46}$.

Polycrystalline $\text{Ba}_8\text{Si}_{46}$ samples were synthesized at high pressure and temperature [13, 18]. The $\text{Ba}_8\text{Si}_{46}$ tips were fabricated by gluing a small grain of the material at the apex of a standard Pt/Ir tip. The grains were then fractured prior TS experiment in order to expose a clean surface facing the STM junction (see inset in Fig.1b). In this work, both ex-situ and in-situ fractured $\text{Ba}_8\text{Si}_{46}$ -tips were studied. As a control of the tip quality, the ability of the tips to image Au or NbSe_2 surfaces was systematically checked. We also visualized the vortex lattice in NbSe_2 and observed the voltage dependent contrast (Fig.1a) expected for high-quality SIS junctions [20]. These evidence both the *vacuum tunneling* regime and the *clean surfaces* of the tunneling electrodes. The raw $I(V)$ data acquired at tunneling resistances 10-100M Ω were numerically derived, and the resulting $dI(V)/dV$ spectra are presented normalized to unity for clarity.

Fig.1b presents typical SIN tunneling conductance spectra obtained with $\text{Ba}_8\text{Si}_{46}$ tips on Au. The spectra exhibit a smooth apparent gap $\Delta_{\text{Ba}_8\text{Si}_{46}} \simeq 1.0$ meV with no additional spectroscopic features visible. The position of the peaks slightly varies (typically ± 0.2 mV) from one

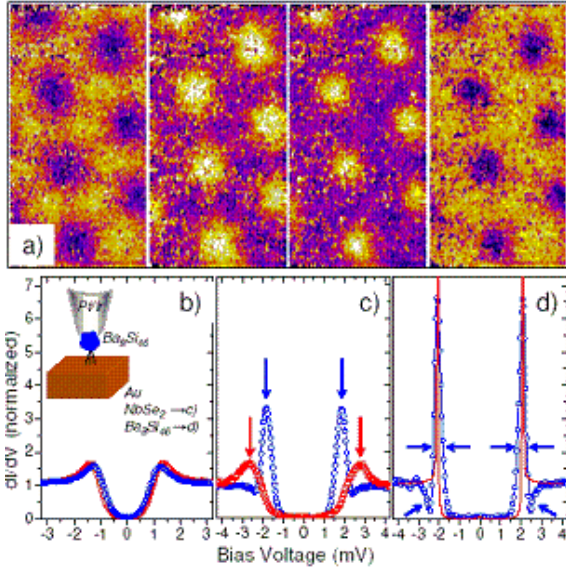


FIG. 1: (Color online) a) Vortex lattice in $NbSe_2$ at $B = 0.165 T$ revealed with Ba_8Si_{46} tips at the biases (from left to right) $-2.0 mV$, $-0.9 mV$, $+1.0 mV$, $+1.9 mV$ shows the contrast inversion characteristic to SIS junctions [20]. b) Two typical SIN tunneling conductance spectra obtained with a Ba_8Si_{46} tips on Au film (red and blue dots). Solid lines: best fits using the McMillan equations (2) with $\Delta_1^0 = 0.08$ (0.05) meV, $\Gamma_1 = 10$ (11) meV, $\Delta_2^0 = 1.2$ (1.33) meV, $\Gamma_2 = 1.49$ (1.31) meV for red (blue) curve; inset - schematic drawing of the experimental geometry. c) Ba_8Si_{46} vs $NbSe_2$ SIS spectra ($T = 2.2 K$) reveal two distinct energy gaps in Ba_8Si_{46} (showed with down arrows): $\Delta_S \approx 0.8$ meV (blue curve) and $\Delta_L \approx 1.4$ meV (red curve). d) Ba_8Si_{46} vs Ba_8Si_{46} SIS tunneling conductance spectrum (blue curve). Red line: SIS fit with BCS clearly fails to reproduce the observed large quasiparticle peaks and dips (pointed with arrows).

grain to another. Such thermally broadened SIN spectra are quite identical to those previously reported [19], and which were interpreted as resulting from the anisotropy of the SC gap. A typical Ba_8Si_{46} - $NbSe_2$ SIS spectrum is presented in Fig.1c (dotted blue curve). In SIS configuration the peaks appear at $\Delta_{peak} = \Delta_{NbSe_2} + \Delta_{Ba_8Si_{46}}$. Considering $\Delta_{NbSe_2}(T = 2.2 K) \simeq 1.1$ meV leads to $\Delta_{Ba_8Si_{46}} \simeq 0.8$ meV. A typical Ba_8Si_{46} - Ba_8Si_{46} SIS spectrum ($T = 2.2 K$) is shown in Fig.1d (dotted blue curve): Its sharpness clearly demonstrates the effect of enhanced energy resolution in SIS tunneling spectroscopy with respect to SIN geometry (Fig1b). The best BCS fit (red solid line in Fig.1d) gives $\Delta_{Ba_8Si_{46}} = 1.04$ meV. Thus, both SIN and SIS data in Fig.1 reveal $\Delta_{Ba_8Si_{46}} = 0.9 \pm 0.2$ meV, too low to account alone for the superconductivity in bulk Ba_8Si_{46} ($2\Delta_{Ba_8Si_{46}}/kT_c = 2.6 < 3.52$). Furthermore, the standard BCS fit (red line in Fig.1d) fails to account for strongly broadened quasiparticle peaks and local minima - dips [21]. Both the low gap energy and the non conventional shape of the tunneling spectra

suggest the existence of another (hidden) leading SC gap Δ_L responsible for the superconductivity in Ba_8Si_{46} .

The necessity of a precise description of realistic SCs stimulated an important piece of theoretical effort. In 1959 Suhl, Matthias and Walker [22] extended the one-band isotropic BCS model to the case of two energy bands. Such a two-band SC exhibits two distinct gaps in its excitation spectrum, Δ_1 and Δ_2 . Analytically, the tunneling DOS is the weighted sum of two BCS spectra $N_{BCSi}(E)$ [1] with two different parameters Δ_1 and Δ_2 :

$$N_S(E) = \sum_{i=1,2} W_i N_{BCSi}(E) = \sum_{i=1,2} W_i N_i(E_F) \frac{|E|}{\sqrt{E^2 - \Delta_i^2}} \quad (1)$$

where W_i is the tunneling probability and $N_i(E_F)$ - the normal state DOS at the Fermi level in each band, $i = 1, 2$. Such $N_S(E)$ does not generate any dip features in SIS spectra and thus, Suhl's model fails to describe our experimental data.

The inter-band quasiparticle scattering, non accounted for in the model above, leads to an additional modification of the quasiparticle excitation spectrum [23]. The latter may be calculated considering two initial BCS gaps in each band Δ_1^0 and Δ_2^0 , and the coupling energies Γ_1 and Γ_2 accounting for the quasiparticle scattering from one band to another. Similarly to the case of the proximity effect in the real space developed by McMillan [24], one obtains two coupled equations for the energy dependent effective gaps $\Delta_1(E)$ and $\Delta_2(E)$:

$$\Delta_1(E) = \frac{\Delta_1^0 + \Gamma_1 \Delta_2(E) / \sqrt{\Delta_2^2(E) - (E - i\Gamma_2)^2}}{1 + \Gamma_1 / \sqrt{\Delta_2^2(E) - (E - i\Gamma_2)^2}} \quad (2)$$

$$\Delta_2(E) = \frac{\Delta_2^0 + \Gamma_2 \Delta_1(E) / \sqrt{\Delta_1^2(E) - (E - i\Gamma_1)^2}}{1 + \Gamma_2 / \sqrt{\Delta_1^2(E) - (E - i\Gamma_1)^2}}$$

These equations allow one to calculate the tunneling spectrum of a two-band SC, by replacing the constant gaps Δ_i in (1) by the energy dependent gaps $\Delta_i(E)$ [25].

In Fig.2a,b we present SIS tunneling spectra, Fig.2c showing their evolution with temperature. The enhanced energy resolution of SIS spectroscopy revealed the apparent gap $\Delta_{Ba_8Si_{46}}$ to vanish exactly at the T_c of the bulk material, thus evidencing its relation to the bulk SC (Fig.2d). The SIS fits using eqs. (2) (solid lines in Fig.2) reproduce in fine details the shape of the SIS tunneling conductance data, with different counter electrode materials (in the case of $NbSe_2$, Fig.2a, the exact DOS was taken from [27]) and at various temperatures (red lines in Fig.2c). A perfect agreement is also achieved when fitting SIN spectra (solid lines in Fig.1b). By analyzing the fitting parameters of different tunneling spectra we noticed the following common features: i) for all spectra initial BCS gap in the band $i = 1$ is $\Delta_1^0 \approx 0$ while $\Delta_2^0 = 1.3 \pm 0.1$ meV. ii) the interband scattering parameters, Γ_1 and Γ_2 strongly vary from one junction to

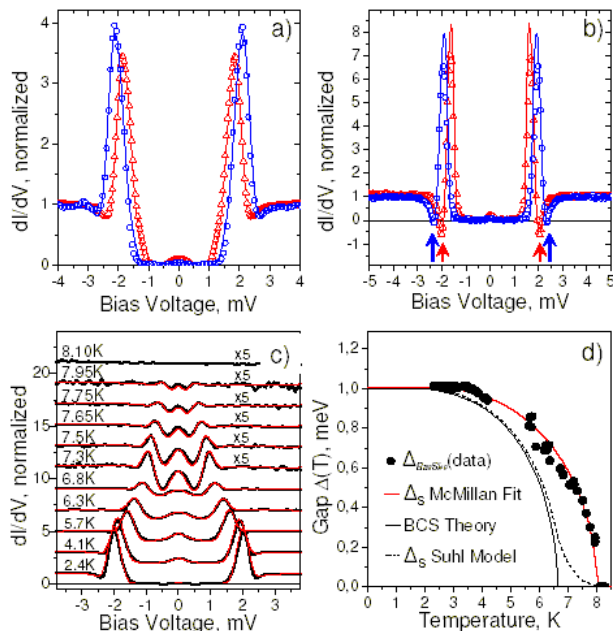


FIG. 2: (Color online) a) and b) Typical SIS tunneling conductance spectra (red and blue dots) observed at $T = 2.2$ K: a) $\text{Ba}_8\text{Si}_{46}$ vs NbSe_2 ; b) $\text{Ba}_8\text{Si}_{46}$ vs $\text{Ba}_8\text{Si}_{46}$. In some junctions a negative tunneling conductance is measured at the dip positions (arrows). Solid lines: best SIS fits with McMillan equations (2) obtained with the following parameters: Red (blue) curve in a): $\Delta_1^0 = 0.0$ (0.07) meV, $\Gamma_1 = 2.2$ (3.54) meV, $\Delta_2^0 = 1.1$ (1.34) meV, $\Gamma_2 = 0.17$ (0.26) meV, the exact DOS of NbSe_2 was taken from [27]; Red (blue) curve in b): $\Delta_1^0 = 0.0$ (0.0) meV, $\Gamma_1 = 2.6$ (3.7) meV, $\Delta_2^0 = 1.1$ (1.23) meV, $\Gamma_2 = 0.18$ (0.40) meV; c) Temperature dependence of $\text{Ba}_8\text{Si}_{46}$ vs $\text{Ba}_8\text{Si}_{46}$ spectra (thick black lines) and their fits with (2) (thin red lines). The spectra are shifted for clarity; d) Comparison of the SIS data in c) with different models.

another, but their ratio remains almost fixed $\Gamma_1/\Gamma_2 \sim 10$ (see also Fig.3d). iii) for most of the studied junctions the tunneling contribution of the band $i = 1$ was $W_1 = 1$ and that of $i = 2$ was $W_2 = 0$, i.e. we needed only the term $N_{S1}(E)$ to fit the tunneling spectra. Thus, only two really free parameters remained, Δ_2^0 and $\Gamma_1(\Gamma_2)$. Moreover, the fits in Fig.2c were generated considering only one free parameter, Δ_2^0 , the second being evaluated at $T = 2.2$ K ($\Gamma_1 = 10$ $\Gamma_2 = 6$ meV) and kept fixed.

Let us now discuss the physics behind such a surprisingly nice agreement between the data and fits, and analyze the consequences of the above mentioned common features. The condition $\Delta_1^0 \approx 0$ meV implies that the superconductivity in the band $i = 1$ is fully induced: a small gap opens in $N_{S1}(E)$ due to the coupling with the leading superconducting band $i = 2$ where the pairing amplitude $\Delta_2^0 \simeq 1.3$ meV is found close to the value 1.4 meV estimated from specific heat measurements [11]. The observed fluctuations of the induced small gap Δ_S from one junction to another, ± 0.2 meV, are attributed

to the variations of both the scattering rates Γ_i and the pairing amplitude of the initial gap Δ_2^0 . Besides, a larger scattering due to the surface disorder may explain the differences between Δ_S observed in TS data and the one (0.35 meV) found in specific heat measurements [11]. Indeed, the value $\Delta_S = 0.35$ meV can be easily calculated with (2) considering a smaller $\Gamma_1 = 0.6$ meV in the bulk.

A clear linear correlation between Γ_1 and Γ_2 is evidenced in Fig.3d, with $\Gamma_1/\Gamma_2 \sim 10$. This result is consistent with the scattering in a two-band material: The interband scattering events $1 \rightarrow 2$ and $2 \rightarrow 1$ should be equal and therefore the condition $\Gamma_1/\Gamma_2 = N_2(E_F)/N_1(E_F)$ must be fulfilled [23]. The ratio ~ 10 we find is in very good agreement with the value $N_2(E_F)/N_1(E_F) = 9$ determined from specific heat measurements [11], that strongly supports our model. Concerning the variations of Γ_1 and Γ_2 observed in different experiments, we relate them to the specific scattering conditions due to the local surface disorder, realized for each junction [28].

In Figs.3a and 3b we show the partial DOSs $N_{Si}(E)$ calculated for bands $i = 1$ and $i = 2$ respectively. We took $\Delta_1^0 = 0$ meV and $\Delta_2^0 = 1.3$ meV, different curves corresponding to the coupling parameters Γ_1 varying from 0.5 to 15 meV with a constant ratio $\Gamma_1/\Gamma_2 = 10$. As a result of the inter-band quasiparticle scattering, a gap Δ_S is induced in the first band where it does not exist at zero coupling. The DOS shape in the first band is very peculiar (Fig.3a): The quasiparticle peaks are broadened and there are some shoulders at the position of the large gap peaks. This peculiar shape is responsible of the dips in SIS spectra, experimentally observed. Broad peaks and dips are also observed in high- T_c SCs and attributed to the coupling with a collective excitation mode [26]. Their amplitudes and the characteristic energies (normalized to the T_c) are however much higher as compared to our case. In the second band, Fig.3b, the initially pure BCS DOS evolves with the coupling: A mini-gap (often called 'excitation gap') appears at the same position that the induced gap in the first band. The evolution of the gaps Δ_L and Δ_S in the partial DOSs with the coupling parameter Γ_1 is presented in Fig.3c. Both gaps vary strongly at moderate Γ_1 and reach the same asymptotic value for very large coupling, where one recovers a simple one-gap BCS DOS.

In the search for a direct evidence of the large gap Δ_L , we studied several tens of $\text{Ba}_8\text{Si}_{46}$ tips and acquired the SIS spectra in thousands of locations, similar to what was done in the case of MgB_2 [29]. We expected that the surface defects such as large steps, protrusions, holes would provide various tunneling conditions. In some measurements we indeed observed very different still reproducible SIS spectra (red curve in Fig.1c), while keeping the tunneling conditions unchanged. They show no dips, as expected for SIS spectra revealing the large gap, Fig.3b. Furthermore, the gap energy $\Delta_L \approx 1.4$ meV correspond-

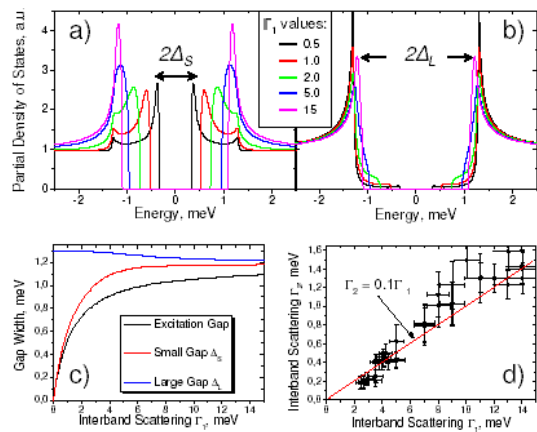


FIG. 3: (Color online) Partial DOSs in the band 1 in (a) and 2 in (b) calculated within the McMillan model with $\Delta_1^0 = 0$, $\Delta_2^0 = 1.3$ meV, $\Gamma_1 = 0.5, 1, 2, 5, 15$ meV, $\Gamma_2 = \Gamma_1/10$. (c) Evolution of the excitation gap and apparent gaps Δ_L , Δ_S with the scattering rate Γ_1 , corresponding to (a) and (b). (d) Scatter plot of the fit parameters Γ_2 vs Γ_1 . Red line: linear dependence $\Gamma_2 = \Gamma_1/10$.

ing to these spectra is in a good agreement with the large gap deduced from specific heat measurements by Lortz et al. [11].

It is not fully established for the moment why the spectra revealing directly the large gap are so rare. In the case of MgB_2 a similar statistics was observed [29] and attributed to the low probability of tunneling into the two-dimensional π -band. It is not clear if such an assumption holds for Ba_8Si_{46} . We know however that in Ba_8Si_{46} most of the DOS belongs to Ba-Si hybridized states located inside the Si cages [17, 18]. It couples well to Ba phonon rattling modes that contribute to the SC pairing [11, 30]. Hence, we may speculate that the electronic states responsible for the superconductivity are somehow confined inside the clathrate cages, and the amplitude of the corresponding evanescent waves outside the material is thus weak, leading to a tiny contribution into the tunneling. Consequently, most of the tunneling current comes from the outer-cage Si orbitals where the superconductivity is purely induced.

Finally, we have studied the quasiparticle excitation spectrum of the superconductor Ba_8Si_{46} by local tunneling spectroscopy. Owing high energy resolution achieved in SIS junctions we resolved fine spectroscopic features that cannot be accounted for by BCS. The SIS spectra evidence the existence of two distinct energy gaps, $\Delta_L = 1.3 \pm 0.1$ meV and $\Delta_S = 0.9 \pm 0.2$ meV, that are interpreted in terms of a two-band superconductivity in Ba_8Si_{46} characterized by a leading gap $2\Delta_L/kT_c = 3.7 \pm 0.3$ and another, smaller coupling-dependent gap Δ_S , reflecting the superconductivity induced in an intrinsically non-superconducting electronic band.

- [1] J. Bardeen, L. N. Cooper, and J. R. Schrieffer, Phys. Rev. **108**, 1175 (1957).
- [2] J.C.F. Brock, Solid State Comm. **7** 1789 (1969).
- [3] V. Guritanu et al., Phys. Rev. B **70**, 184526 (2004) and refs. therein.
- [4] Lawrence Yun Lung Shen, N. M. Senozan and Norman E. Phillips, Phys. Rev. Lett. **14**, 1025 (1965).
- [5] F. Bouquet et al., Europhys. Lett. **56**, 856 (2001).
- [6] F. Giubileo et al., Phys. Rev. Lett. **87**, 177008 (2001)
- [7] G. Rubio-Bollinger *et al.*, Phys. Rev. Lett. **86**, 5582 (2001); P. Szabó *et al.*, Phys. Rev. Lett. **87**, 137005 (2001).
- [8] B. Bergk et al., Phys. Rev. Lett. **100**, 257004 (2008) and references therein.
- [9] C. Dubois et al., Phys. Rev. B **75**, 104501 (2007).
- [10] I. Guillamon et al., Phys. Rev. Lett. **101**, 166407 (2008).
- [11] Lortz et al., Phys. Rev. B **77**, 224507 (2008).
- [12] A. San Miguel and P. Toulemonde, High Pressure Research **25**, 159 (2005).
- [13] P. Toulemonde, Ch. Adessi, X. Blase, A. San Miguel and J. L. Tholence, Phys. Rev. B **71**, 094504 (2005).
- [14] H. Kawaji, H. Horie, S. Yamanaka, and M. Ishikawa, Phys. Rev. Lett. **74**, 1427(1995).
- [15] S.Yamanaka et al. Inorg. Chem. **39**, 56 (2000).
- [16] Connétable et al. Phys. Rev. Lett. **91**, 247001 (2003).
- [17] K. Tanigaki et al., Nature Materials **2**, 653 (2003).
- [18] P. Toulemonde et al., Journal of Physics and Chemistry of Solids **67**, 1117 (2006).
- [19] K. Ichimura, K. Nomura, H. Fukuoka and S. Yamanaka, Physica C **388-389**,577 (2003)
- [20] A. Kohen et al., Phys. Rev. Lett. **97**, 027001 (2006).
- [21] Note that Ba_8Si_{46} - Ba_8Si_{46} junctions do not contain any host material (as it is the case of Ba_8Si_{46} - $NbSe_2$ junctions). Thus, the observed deviations from BCS behavior are intrinsic to Ba_8Si_{46} .
- [22] H. Suhl, B. T. Matthias, and L. R. Walker, Phys. Rev. Lett. **3**, 552 (1959).
- [23] N. Schopohl, K. Scharnberg, Solid State Commun. **22**, 371 (1977)
- [24] W. L. McMillan, Phys. Rev. **175**, 537 (1968).
- [25] Applied to the case of MgB_2 this formalism already gave a nice agreement with the experimental results (H. Schmidt, J.F. Zasadzinski, K.E. Gray and D.G. Hinks, Physica C **385**, 221 (2003)).
- [26] P. Romano et al. Phys. Rev. B, 092514 (2006) and refs. therein.
- [27] J.G. Rodrigo and S. Vieira, Physica C **404**, 306 (2004).
- [28] Note that the surface itself is a topological defect with respect to the bulk material, due to the crystal symmetry breaking. It could in principle result in a new electronic band, present only at the surface (as it is the case of Cu(111) or Ag(111), for instance). The superconductivity could be induced to this band by the coupling with the bulk SC, and thus, Δ_S could, in principle, represent the surface state SC gap which would not extend to the bulk. Such hypothesis is generally valid for the surface of any SC, and cannot be ruled out even for in-situ prepared junctions. However, we did not find any evidence for such a surface band.
- [29] F. Giubileo, D. Roditchev, W. Sacks, R. Lamy and J. Klein, Europhys. Lett., **58**, 764 (2002).

[30] J.S. Tse et al., Phys. Rev. B, **72**, 155441 (2005).